Impact of Battery State of Charge on In-Situ Power Line Communication within an Intelligent Electric Vehicle

Mahyar J. Koshkouei, Erik Kampert, Andrew D. Moore, and Matthew D. Higgins

Abstract— **Real-time communication of high-fidelity data can lead to significant improvements of the performance and safety of batteries used in intelligent electric transportation. Power line communication (PLC) may be used by smart instrumented cells to network within a battery pack, as well as with an external battery management system as part of battery electric vehicles and smart grids. This paper studies the effectiveness of a PLC system through a Lithium-ion cell as a communication channel, when it is at 5 %, 40 %, 60 %, and 80 % state of charge (SoC). High bit-rate communication is realised through the use of quadrature amplitude modulation up to 1024-QAM and for carrier frequencies from 10 MHz to 200 MHz. The obtained results illustrate that in particular a SoC of 80 % has a significant impact on the communication performance at specific frequencies for 256, 512, and 1024-QAM. The impact of cell state of charge on an in-situ PLC system is analysed in detail, and recommendations on the parameters of such system based upon experimental results are provided.**

I. Introduction

Battery electric vehicles (BEVs) are receiving much attention as an alternative to traditional internal combustion engine vehicles due to their reduced impact on the environment, if charged using renewable energy. However, in comparison, BEVs are relatively limited in their energy density, driving distance on a single charge, long charging time, and running costs [1]. Further research and technologies are required in order to solve these limitations and disadvantages [2].

The performance of the energy storage system with BEVs can directly impact the driving distance and charging time. The Lithium-ion (Li-ion) cell is typically selected for use within such energy storage systems due to its advantages and capabilities, such as capacity and power density, over alternative cell technologies. An in-depth comparison between these cell technologies and their advantages and limitations is provided by [3]. The full potential of the Li-ion cell has yet to be explored due to its sensitivity to internal temperature. Hence, working voltages and charge/discharge rates are limited to mitigate reduction in lifetime, performance, and safety [4]. A battery management system (BMS) is therefore typically used within Li-ion battery packs as it offers performance and safety features, including cell balancing and charge rate control [5]. Existing work on improving the performance of the Li-ion cell includes the optimisation of depth of discharge [6], and estimation of Li-ion cell state of charge (SoC) and state of health [7].

The performance and safety of the Li-ion battery pack can be further enhanced by utilising instrumented cells that have integrated sensors, or 'smart cells' which additionally use an embedded system. These techniques offer improvements to the performance and safety of BEV energy storage systems. Such improvements include the use of internal temperature sensor data and embedded computer systems for enhanced characterisation and performance of the cell at real-time [8].

Instrumented cells are currently limited in their functionality due to either their functioning as a system independent of other cells within the battery pack, or requiring a separate wiring harness to communicate with other smart cells in the battery pack and to the external BMS. Instead, this means that the smart cell must make estimations on the characteristics of the other cells within the battery pack. To increase the potential advantages of a smart cell system, a communication system can be utilised to communicate in-situ sensor data with other smart cells and the BMS to make improved decisions on power management and fault mitigation.

A power line communication (PLC) system enables the power network to be additionally used as a communication channel. It therefore eliminates the need for a specific wiring harness for communication, as the existing power bus bar within the battery pack is utilised [9], [10]. Existing research on the effectiveness and limitations of in-situ PLC within a Li-ion battery pack and its dependence on SoC is limited.

The use of PLC within an energy storage system allows for unprecedented improvements in energy storage system design, safety, performance, real-time diagnostics of smart cells to the BMS, as well as the extension of this PLC network beyond the energy storage system to a BEV or smart grid. A high-level diagram depicting the PLC-connections between these systems is presented in Fig. 1. As stated in [11], these methods allow for real-time system improvements, including:

1) Recommendations of driving behaviour that benefit the longevity and performance of the battery.
2) Automatic vehicle and battery safety analysis and actions.
3) Local and remote diagnosis of the battery, and each smart cell within, by the user and manufacturer.
4) Smart grid power management using vehicle-to-grid technology such as charge scheduling.
5) Individual diagnosis of cells using smart cell to smart grid communication via Internet of Things (IoT) connections.

All authors are with WMG, University of Warwick, Coventry, UK.
Corresponding author: mahyar.koshkouei@warwick.ac.uk

The data that support the findings of this study are openly available in the Warwick Research Archive Portal (WRAP) at: https://wrap.warwick.ac.uk/163448.

*This work was supported in part by the UK Engineering and Physical Sciences Research Council (EPSRC) (Grant no. EP/N509796/1 and EP/R513374/1), and in part by the WMG centre High Value Manufacturing Catapult, University of Warwick, Coventry, UK.

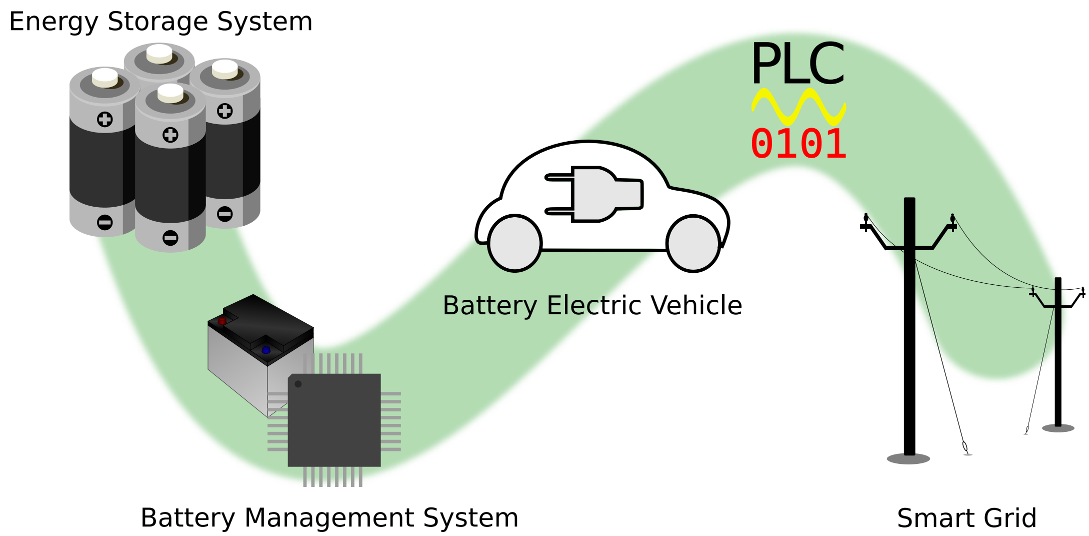

Fig. 1. High-level overview of various vehicular systems and services connected by PLC, with the bidirectional PLC network shown in green. The focus of this work is on the energy storage system.

SoC is a measurement of a batteries' remaining level of charge. Previous studies show that the impedance of a Li-ion cell changes with SoC [12]. However, these works only perform impedance measurements for the relatively low frequency range from 100 mHz to 100 kHz. Therefore, further research is required into measuring the changes in Li-ion cell impedance at higher frequencies, that are suitable for use within higher throughput communication systems. Changes in impedance will result in changes to attenuation and phase shift of the transmitted signal. In this study, these challenges are considered.

In this paper, the effectiveness of PLC on a Li-ion cell at various SoC and at a range of carrier frequencies is evaluated. Furthermore, the use of quadrature amplitude modulation (QAM) is tested for its support of high data rates and effectiveness in noise rejection. This work therefore evaluates modulations of PLC on a Li-ion cell that are similar to those used in vehicle-to-everything (V2X) and dedicated short-range communication (DSRC) in order to streamline a future communication path with existing external systems or infrastructure, such as a smart grid.

The key contributions of this paper are:

1) Analysis and comparisons of the communication performance of QAM with PLC on an 18650-model Li-ion cell with a SoC of 5 %, 40 %, 60 % and 80 %, and carrier frequencies in the range from 10 MHz to 200 MHz.
2) Recommendations of communication parameters on carrier frequency and QAM order based upon this study and empirical facts.

This paper is organised as follows: Section II addresses the methodology of the SoC experimentation, Section III presents the experimental results and their analysis, and Section IV provides conclusions and appropriate recommendations on PLC parameters based on the presented, verified results and additional empirical facts.

II. Experimental Details

The experimental work utilises a NI PXIe-5840 vector signal transceiver (VST) to transmit and receive QAM symbols at a configured carrier frequency. For each carrier frequency tested, the symbol trace and the error vector magnitude (EVM) are collected from the transceiver. The symbol trace is demodulated to bits of data, and is compared with known data transmitted to calculate the bit error rate (BER) and the symbol error rate (SER).

This work consists of four experiments, whereby the Li-ion cell under test is subsequently charged to the voltage that corresponds to the SoC required. To determine the changes in RMS EVM and SER when the battery is in moderate use, 40 %, 60 % and 80 % SoC will be tested. In addition, 5 % SoC is tested to determine the Li-ion cell characteristics when in a fully discharged state. Once the cell is charged to within ±2 % of the desired SoC, it is disconnected from the charging apparatus and left to cool to room temperature for at least one hour before reconnecting the cell to the experimental circuit and commencing the experiment.

During each experiment, a sweep of carrier frequencies from 10 MHz to 200 MHz at a step of 1 MHz is performed for each QAM order of 4, 16, 32, 64, 128, 256, 512, and 1024-QAM. For all experiments, 100,000 symbols are transmitted, such that the first set of symbols is a sequence of training symbols required for the VST to perform phase shift compensation and auto-gain filtering. The remaining symbols are known random data. The number of symbols transmitted remains constant for each QAM order tested. However, since the number of bits within each symbol increases with QAM order, the number of data bits transmitted increases also with higher tested QAM order. An output power of −9 dB m is selected for the transmitted signal to accommodate for maximum signal attenuation by the Li-ion cell, but remain well below the level at which the VST warns for ADC overloading and waveform clipping.

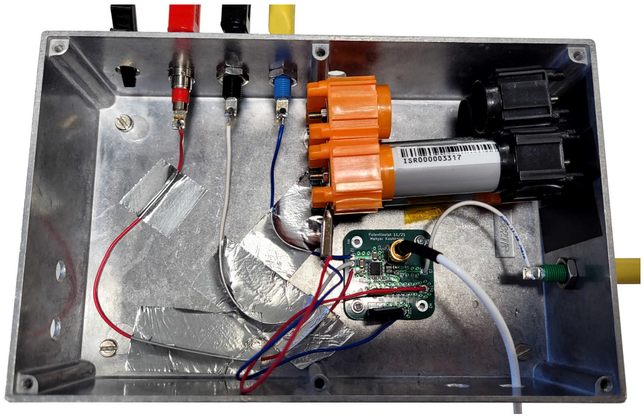

Fig. 2. Photo of the Li-ion cell, DC offset circuit, and resistor within the Faraday shield.

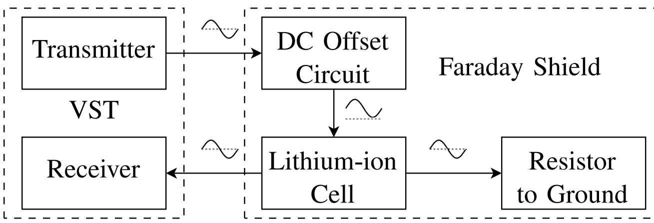

Fig. 3. Overview of connections within experiment. The propagation of signals through the system are shown.

The VST is connected to the Li-ion cell via a DC offset circuit that applies a DC offset to the transmitted signal, equal to the voltage of the connected cell. This protects the VST from overloading and related permanent damage. A very high frequency and high current operational amplifier is used to apply this DC offset, to ensure that the transmitted signal is unaltered. The DC offset signal is connected to the positive terminal of the cell, with the negative terminal of the cell connected to both the receiver of the VST and to a thick-film resistor, as shown in Fig. 3. The cell, DC offset circuit, and the resistor are all placed within a Faraday shield to reduce the influences of external electromagnetic interference, as shown in Fig. 2. Accordingly, the VST and the Faraday shield are connected via 12.4 GHz double-braid shielded SMA cables which are of *RG-316 DS* model manufactured by Cinch Connectivity Solutions.

The EVM data acquired for each carrier frequency tested, are calculated by measuring the difference in the magnitude of the deviations between the received QAM constellation and the expected reference constellation. The results of the EVM presented in Section III are described as an average, as the VST performs oversampling at eight times the symbol rate.

Moreover, the received demodulated data bits are compared with the transmitted data bits to obtain the BER, which is a ratio of erroneous bits against the total number of bits transmitted. The SER is a ratio of erroneous symbols, whereby an erroneous symbol may contain a single erroneous bit up to all incorrect bits. The effect of an erroneous bit is therefore larger for SER than for BER. The measurement BER-data

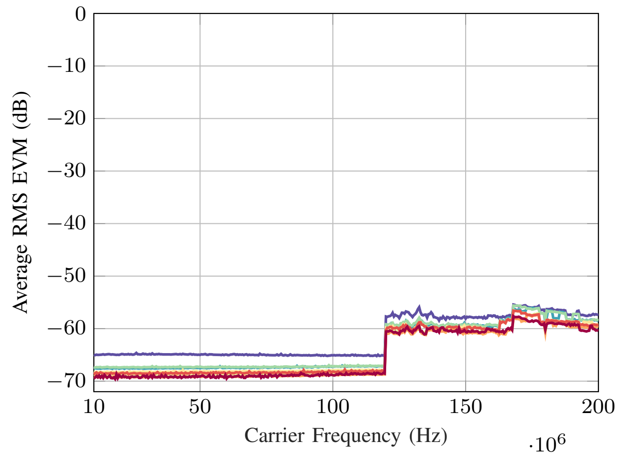

Fig. 4. Average RMS EVM for various QAM-signals with the transmitter and the receiver directly connected.

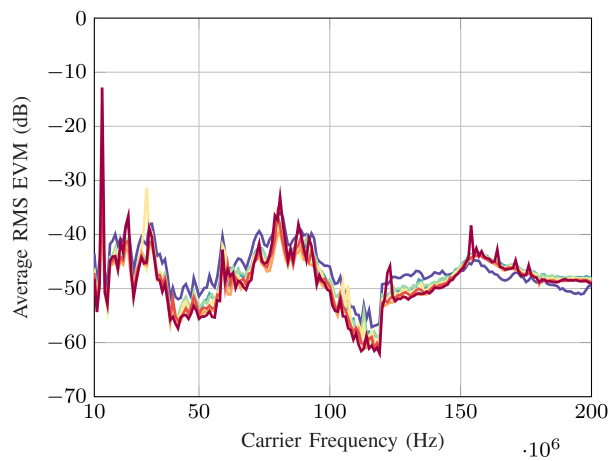

Fig. 5. Average RMS EVM for various QAM-signals through the copper core.

are not separately presented in this paper, as they do not significantly differ from the obtained SER.

The Li-ion cells used in the experiments are of an NCR18650BD model manufactured by Panasonic. In total, four cells of the same model were individually tested and have illustrated almost indistinguishable results. For brevity purposes, the results for a single cell are presented here.

This research aims to show how changes in SoC can affect a PLC system across a Li-ion cell for various carrier frequencies. Using EVM data, it will be possible to understand the potential impact SoC may have on the communication system. Furthermore, the BER and SER are analysed to conclude whether this impact on EVM is sufficiently significant to cause any data corruption within the communication system. Various QAM orders are tested to demonstrate how higher bit rate communication may be achieved, and to give conclusions about the most appropriate parameters for the system based upon the experimental results presented.

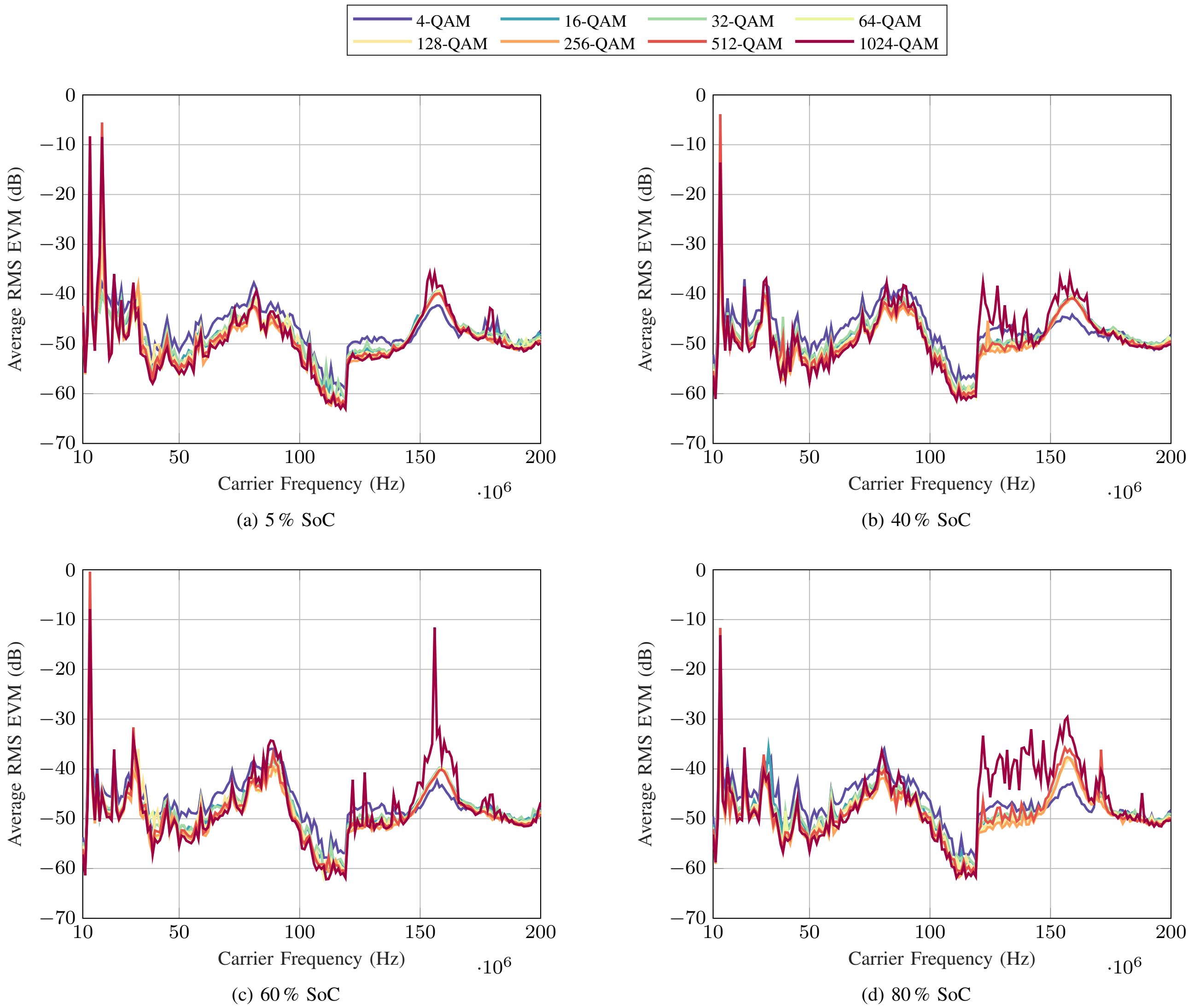

Fig. 6. Average RMS EVM for QAM-signals transmitted through the Li-ion cell at various SoC.

III. Results and Discussion

A. EVM

To first measure the minimum EVM possible, the output of the VST is directly connected to the input. The resulting measurements are presented in Fig. 4, which shows that for all QAM orders tested, the EVM remains below −64.6 dB up to a carrier frequency of 120 MHz, and then rises to a maximum of −55.3 dB above 120 MHz. This performance occurs because the VST adds a "local oscillator driven mixing stage" to the RF signal path for carrier frequency configurations for 120 MHz and above [13]. This EVM-baseline can be compared with the EVM acquired when the VST is connected to the experiment environment. Figure 5 displays the EVM when the VST is connected to the experimental circuit with a multi-strand bare copper wire cable core, with a total diameter of 16 mm connected within the cell holder. By comparing these results with those acquired with the cell under test, one can deduce the effects that the cell alone has on the communication system.

The average RMS EVM for PLC through a Li-ion cell at the SoC tested is presented in Fig. 6. A general trend can be seen in all four results, whereby a sharp peak appears at 13 MHz, with two smaller local maxima near 85 MHz and at 159 MHz. The sudden increase in EVM at 120 MHz is attributed to the change in signal path as already stated. In contrast to the EVM of the copper core as shown in Fig. 5, the maximum at 90 MHz is attenuated and the maximum at 159 MHz is larger for all SoC tested.

For every SoC, it can be observed that 1024-QAM results in the highest EVM for carrier frequencies higher than 121 MHz, whereas for frequencies smaller than 121 MHz, 4-QAM shows marginally higher EVM. However, it is also indicated that at 80 % SoC, the EVM for 1024-QAM increases and remains above −40.0 dB for carrier frequencies between 121 MHz and 163 MHz. A maximum of −11.6 dB EVM can be seen with 1024-QAM at 156 MHz with a SoC of 60 %. This feature can also be observed with 5 % and 40 % SoC, but with decreased

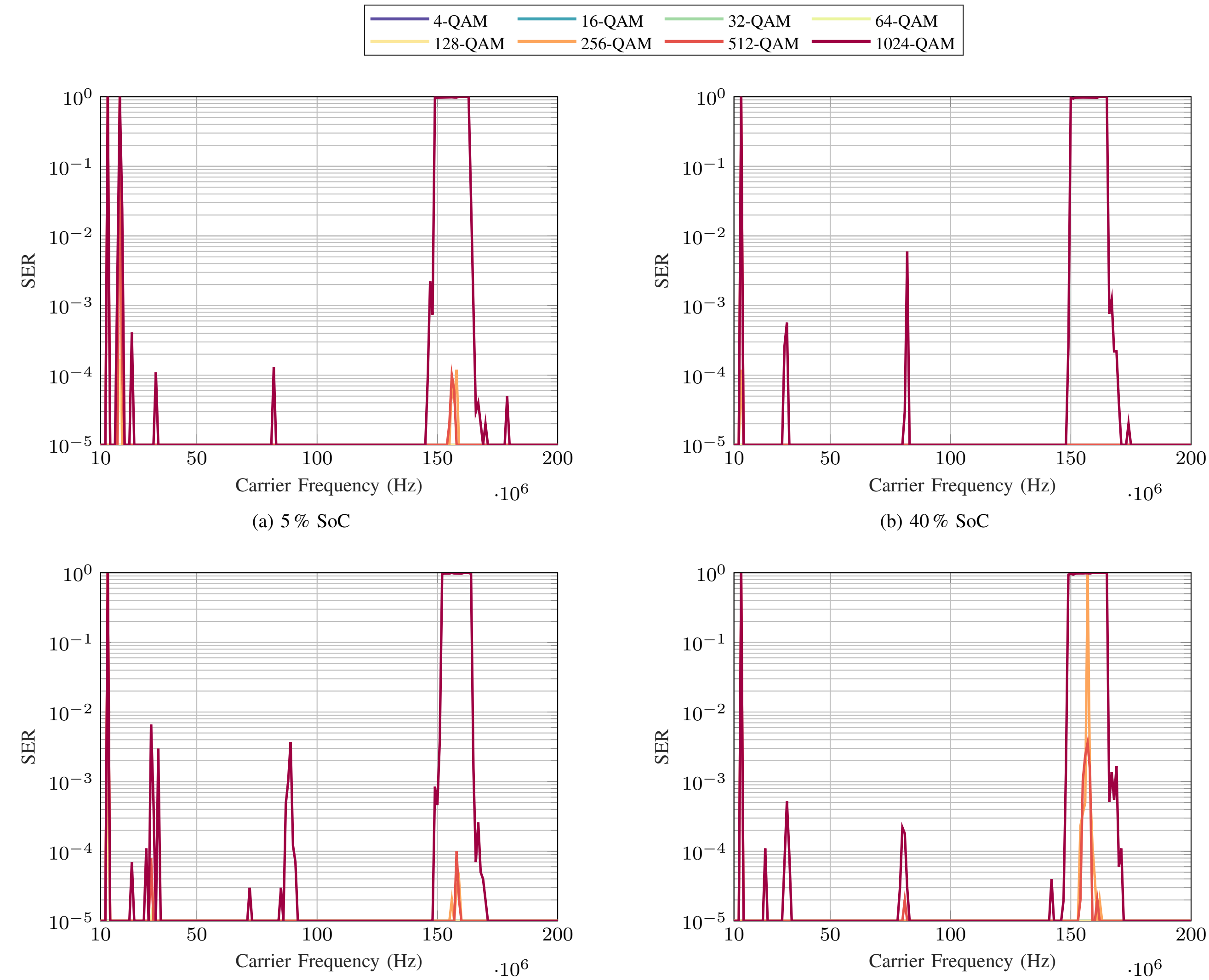

(a) 5 % SoC

(b) 40 % SoC

(c) 60 % SoC

(d) 80 % SoC

Fig. 7. SER ratio for various QAM-signals transmitted through Li-ion cell at various SoC.

magnitude and for a narrower frequency range. Moreover, a peak in EVM is also visible for all SoC and QAM orders at 13 MHz.

At 156 MHz, the EVM of 512-QAM increases to −35.8 dB at 80 % SoC. This is in contrast to the other SoC tested, whereby the EVM of 512-QAM signals are below −40.0 dB at −40.1 dB, −41.8 dB, and −41.5 dB for 5 %, 40 %, and 60 % SoC, respectively.

B. SER

The results for SER as presented in Fig. 7 highlight that symbol errors occur for 256, 512 and 1024-QAM. In fact, 1024-QAM produces the most symbol errors, which appear at a larger number of carrier frequencies, reaching an SER 1.0 at 13 MHz and within the wide frequency range of 145 MHz to 172 MHz.

Alterations in the magnitude of SER between the different SoC tested occur between carrier frequencies of 154 MHz and 162 MHz. Using 256 and 512-QAM, the cell at 5 % and 60 % SoC display a similar SER of 1.2×10^{-4} and 1.0×10^{-4} at 158 MHz, respectively. No increase in SER is detected when the cell is at 40 % SoC. In contrast, the cell at 80 % SoC demonstrates worse communication performance, whereby the SER for 256 and 512-QAM rises to 0.94 and 3.6×10^{-3}, respectively. This local maximum in SER for 256-QAM may be attributed to corrupted training symbols, causing the remaining of the symbols in the data received to be demodulated incorrectly.

Upon comparison with the obtained EVM data in Fig. 6, it can be observed that the SER for 256 and 512-QAM increases as the magnitude of EVM rises above −40.0 dB. The rise to −36.1 dB at 158 MHz with 512-QAM and 80 % SoC as shown in Fig. 6d, corresponds with the significant increase in SER at the same carrier frequency. At 5 % and 60 % SoC, the EVM for both 256 and 512-QAM at 158 MHz reaches −39.9 dB. In comparison, at 40 % SoC, the EVM for both 256 and 512-QAM approaches only −40.9 dB. It can therefore be concluded that when utilising a carrier frequency between 154 MHz to 162 MHz, an EVM of at least −40.0 dB is required when using 256 or 512-QAM to mitigate errors in the symbols received.

For modulation orders smaller than 256-QAM, no erroneous symbols are observed for all carrier frequencies and SoC tested. This is because the higher modulation orders require a lower EVM due to the increased number of symbols within the same constellation space. Hence, established communication system standards provide minimum EVM thresholds when using QAM [14].

By combining the EVM and SER results, it can be interpreted that the most appropriate carrier frequencies for a PLC system through a Li-ion cell are in the ranges of 40 MHz to 65 MHz and 95 MHz to 140 MHz. At these carrier frequencies, the change in SoC does not have negative effects on the communication system for all QAM orders tested, for a certain minimum output power. For other carrier frequencies, modulation orders of 128-QAM and lower, may be used as they do not produce any symbol errors due to their increased tolerance against high EVM.

We have reported previously that when multiple Li-ion cells are connected within a battery configuration, the performance of an in-situ PLC system also changes [15]. As such, the configuration of the battery must be taken into account in addition to the changes in performance due to SoC of the cells within the battery. Therefore, the following properties are required to guarantee the performance of a communication system for use within a Li-ion battery that is not impaired by changes in SoC: a lower QAM order; a carrier frequency with reduced EVM; and use of signal conditioning techniques such as phase shift compensation and auto-gain filtering.

IV. Conclusions

This paper has investigated how the state of charge (SoC) of an energy storage system may affect a power line communication (PLC) system. Such a system allows smart cells to communicate real-time diagnostic data with other smart cells, to the battery management system (BMS), and may be further extended to communicate with existing battery electric vehicles (BEV) or smart grid networks, in order to facilitate improvements in performance, safety, and coordination.

An 18650 model Li-ion cell has been tested at different SoC of 5 %, 40 %, 60 %, and 80 %, to investigate its effects on an in-situ PLC system that utilises quadrature amplitude modulation (QAM) for carrier frequencies between 10 MHz and 200 MHz. The obtained results have illustrated that the SoC has a significant impact on communication performance at specific frequencies for 256, 512, and 1024-QAM. In particular, a SoC of 80 % has the strongest negative impact on the PLC system. Therefore, it can be concluded that the most appropriate PLC parameters for a desired system are carrier frequencies between 40 MHz and 65 MHz or 95 MHz and 140 MHz, and utilising a modulation order of 256-QAM or lower. With these parameters, the performance of the communication system is not affected by any alterations in SoC.

For large-scale Li-ion battery configurations, such as those in use within BEVs, it is recommended that a lower QAM-order and signal conditioning techniques are utilised. This will mitigate the propagation of error caused by the alterations in SoC of the individual cells within the battery pack on the performance of the communication system as a whole.

Ongoing work includes communication error analysis in terms of bit and symbol error ratios for carrier frequencies up to 6 GHz, and the evaluation of distinct Li-ion battery pack configurations in order to determine their suitability and limitations for a large-scale system.

References

[1] J. N. Barkenbus, "Prospects for electric vehicles," *Sustainability*, vol. 12, no. 14, p. 5813, Jul. 2020.

[2] B. Lebrouhi, Y. Khattari, B. Lamrani, M. Maaroufi, Y. Zeraouli, and T. Kousksou, "Key challenges for a large-scale development of battery electric vehicles: A comprehensive review," *Journal of Energy Storage*, vol. 44, p. 103273, Dec. 2021.

[3] D. Andrea, *Battery Management Systems for Large Lithium Battery Packs*. Artech House Publishers, Sep. 2010.

[4] F. Arshad, J. Lin, N. Manurkar, E. Fan, A. Ahmad, M. un Nisa Tariq, F. Wu, R. Chen, and L. Li, "Life cycle assessment of lithium-ion batteries: A critical review," *Resources, Conservation and Recycling*, vol. 180, p. 106164, May 2022.

[5] K. Liu, K. Li, Q. Peng, and C. Zhang, "A brief review on key technologies in the battery management system of electric vehicles," *Frontiers of Mechanical Engineering*, vol. 14, no. 1, pp. 47–64, Apr. 2018.

[6] C. Reiter, N. Wassiliadis, L. Wildfeuer, T. Wurster, and M. Lienkamp, "Range extension of electric vehicles through improved battery capacity utilization: Potentials, risks and strategies," in *2018 21st International Conference on Intelligent Transportation Systems (ITSC)*. IEEE, Nov. 2018.

[7] Y. Gao, K. Liu, C. Zhu, X. Zhang, and D. Zhang, "Co-estimation of state-of-charge and state-of- health for lithium-ion batteries using an enhanced electrochemical model," *IEEE Transactions on Industrial Electronics*, vol. 69, no. 3, pp. 2684–2696, Mar. 2022.

[8] T. Amietszajew, E. McTurk, J. Fleming, and R. Bhagat, "Understanding the limits of rapid charging using instrumented commercial 18650 high-energy li-ion cells," *Electrochimica Acta*, vol. 263, pp. 346–352, Feb. 2018.

[9] T. A. Vincent, B. Gulsoy, J. E. H. Sansom, and J. Marco, "A smart cell monitoring system based on power line communication—optimization of instrumentation and acquisition for smart battery management," *IEEE Access*, vol. 9, pp. 161 773–161 793, 2021.

[10] V. Marsic, T. Amietszajew, P. Igic, S. Faramehr, and J. Fleming, "DC power line communication (PLC) on 868 MHz and 2.4 GHz wired RF transceivers," *Sensors*, vol. 22, no. 5, p. 2043, Mar. 2022.

[11] A. Amin, W. U. K. Tareen, M. Usman, H. Ali, I. Bari, B. Horan, S. Mekhilef, M. Asif, S. Ahmed, and A. Mahmood, "A review of optimal charging strategy for electric vehicles under dynamic pricing schemes in the distribution charging network," *Sustainability*, vol. 12, no. 23, p. 10160, Dec. 2020.

[12] T. Chen, M. Huo, X. Yang, and R. Wen, "A fast lithium-ion battery impedance and SOC estimation method based on two-stage PI observer," *World Electric Vehicle Journal*, vol. 12, no. 3, p. 108, Aug. 2021.

[13] NI. (2022, Jan.) Interconnecting multiple pxie-5840 rf channels (homogeneous channel types). [Online]. Available: https://zone.ni.com/reference/en-XX/help/373680F-01/vstdevices/interconnecting_multiple_5840_rf_channels/

[14] "IEEE standard for information technology–telecommunications and information exchange between systems - local and metropolitan area networks–specific requirements - part 11: Wireless lan medium access control (MAC) and physical layer (PHY) specifications," *IEEE Std 802.11-2020 (Revision of IEEE Std 802.11-2016)*, pp. 1–4379, 2021.

[15] M. J. Koshkouei, E. Kampert, A. D. Moore, and M. D. Higgins, "Evaluation of an in situ QAM-based power line communication system for lithium-ion batteries," *IET Electrical Systems in Transportation*, Jun. 2021.